Large-volume results in SU(2) with adjoint fermions

L. Del Debbio[∗]

The Higgs Centre for Theoretical Physics
The University of Edinburgh, Edinburgh, UK
E-mail: Luigi.Del.Debbio@ed.ac.uk

B. Lucini

College of Science
Swansea University, Swansea, UK
E-mail: b.lucini@swansea.ac.uk

C. Pica

CP^3-Origins & the Danish IAS,
University of Southern Denmark, Odense, Denmark
E-mail: pica@cp3.dias.sdu.dk

A. Patella

PH-TH, CERN, Geneva, Switzerland, and
School of Computing and Mathematics & Centre for Mathematical Science,
Plymouth University, Plymouth UK
E-mail: agostino.patella@plymouth.ac.uk

A. Rago

School of Computing and Mathematics & Centre for Mathematical Science,
Plymouth University, Plymouth UK
E-mail: antonio.rago@plymouth.ac.uk

S. Roman

The Higgs Centre for Theoretical Physics
The University of Edinburgh, Edinburgh, UK
E-mail: S.Roman@ed.ac.uk

Taming finite-volume effects is a crucial ingredient in order to identify the existence of IR fixed points. We present the latest results from our numerical simulations of SU(2) gauge theory with 2 Dirac fermions in the adjoint representation on large volumes. We compare with previous results, and extrapolate to thermodynamic limit when possible.

[∗]Speaker.

1. Introduction

Motivated by the possible existence of a strongly-interacting sector beyond the Standard Model, extensive studies of vector gauge theories have been recently performed, for varying number of colors, flavors, and representation of the matter fields – see Kuti's talk in these proceedings for a recent summary of results [1]. A realistic candidate for BSM phenomenology must satisfy the constraints from electroweak precision data, and lead to a successful construction of the SM flavor sector. It has been clear for a long time that a rescaled version of QCD would not be adequate, and several investigations have focussed on finding theories characterized by a large separation between the IR and UV scales. Confining theories close to the edge of the conformal window are believed to satisfy this requirement; the RG evolution of the couplings is very slow (*walking*), which in turn leads to an approximate scale invariance at large distances. Gauge theories with matter in higher representations could lead to this type of behaviour as argued in Ref. [2]. Unfortunately a sharp characterization of walking behaviour has proved elusive so far, despite some encouraging numerical evidence, see e.g. Refs. [3, 4, 5] for the latest papers, and citations therein.

Proving the existence of an infrared fixed point (IRFP) is a well-defined question, for which we can hope to find an unambiguous answer. Phenomenologically relevant models could then be defined by deformations of the conformal theory, as suggested in Ref. [6]. The low-energy dynamics is then characterized by the anomalous dimensions of the relevant operators at the putative IRFP. It has been known since the pioneering work in Ref. [7] that large anomalous dimensions are required in order to construct phenomenologically viable models. There are interesting bounds between these anomalous dimensions that should be studied in more detail [8]. Finally it is worthwhile to recall that realistic models have been constructed recently from a holographic approach [9]. These studies should be complementary to the lattice ones presented in this work.

The work reported here is part of our ongoing investigation of the existence of an IRFP in the SU(2) gauge theory with two Dirac fermions in the adjoint representation, which is also known under the name of Minimal Walking Technicolor (MWT) [10]. This model is believed to have a fixed point [12, 13, 11], and we would like to obtain more quantitative results in particular about the mass anomalous dimension at the IRFP. The systematic errors of lattice simulations need to be kept under control in order to highlight the interesting conformal behaviour. Previous studies, which have been useful in the early stages of the numerical investigations, are clearly affected by large systematics and are useless in order to understand the physics of these theories.

In this note, we concentrate on the study of the spectrum of MWT. The systematic errors due to the finite temporal and spatial extents of the lattice have been analysed in previous publications, see e.g. Ref. [14], where we found that systematic errors of approximately 10% are common on lattices such that $M_{PS}L < 10$, where M_{PS} indicates the mass of the lightest pseudoscalar state in the meson spectrum. We have therefore embarked in large volume simulations of the theory, in order to obtain results for the spectrum in a regime where systematic errors are below 1%.

The new volumes simulated are large enough to avoid finite temperature effects, and to allow an extrapolation of the spectrum to the infinite volume limit for two values of the fermion mass. These are the first results for the spectrum of the MWT that can be extrapolated to the thermodynamical limit with an uncertainty at the percent level. The results for the full spectrum, including glueball states, and the string tension, are discussed in Sect. 3.

2. Methodology

We have simulated MWT using the RHMC algorithm described in Ref. [15]. In order to iden-
tify, and control, the systematic effects due to the finite size of the lattices, we have simulated the
theory on a series of lattices, increasing both the temporal and the spatial extent of the system. All
simulations have been performed at fixed lattice bare coupling $\beta = 2.25$, and for two values of
the fermion bare mass $am_0 = -1.05, -1.15$. We have also compared the spectrum obtained from
simulations with the usual periodic boundary conditions, to the one obtained with twisted bound-
ary conditions, as defined in Ref. [16]. The details of our implementation will be presented in a
forthcoming publication. In the infinite volume limit, results should be independent of the boun-
day conditions, and therefore we can use the dependence on the boundary conditions to monitor
whether or not the theory has reached the large volume asymptotic behaviour. The new runs are
listed in Tab. 1.

lattice	V	$-am_0$	N_{traj}	t_{traj}	$\langle P \rangle$	τ	λ	τ_λ
A10	64×8^3	1.15	810	3	0.66536(22)	3.6(1.2)	0.2005(58)	1.42(31)
A11	64×12^3	1.15	530	1.5	0.66601(15)	1.93(59)	0.2054(40)	1.54(43)
C5	64×16^3	1.15	1500	1.5	0.665992(61)	2.32(46)	0.2116(16)	2.38(48)
D4	64×24^3	1.15	2387	1.5	0.665927(26)	3.92(79)	0.21478(70)	1.70(24)
F1	64×32^3	1.15	2541	1.5	0.665946(30)	3.37(62)	0.2115(12)	1.06(12)
G1	80×48^3	1.15	2200	1.5	0.665943(17)	5.1(1.2)	0.2237(17)	0.637(58)
B2	24×12^3	1.05	7819	1	0.647633(70)	6.79(99)	1.4936(51)	5.80(78)
C6	64×16^3	1.05	2648	1.5	0.647645(48)	4.63(96)	1.4389(36)	1.26(14)
D5	64×24^3	1.05	4000	1.5	0.647695(37)	3.56(53)	1.3906(45)	0.722(54)
F2	48×32^3	1.05	3590	1.5	0.647680(30)	4.28(74)	1.3708(49)	0.632(45)
TWA1	64×8^3	1.15	565	1.5	0.66665(22)	2.8(1.0)	0.5557(96)	0.85(18)
TWB1	64×12^3	1.15	741	1.5	0.66590(11)	2.96(96)	0.2709(48)	1.93(50)
TWC1	64×16^3	1.15	1162	1.5	0.665990(61)	2.91(73)	0.2484(17)	6.2(2.2)
TWD1	64×24^3	1.15	2701	1.5	0.665912(35)	4.63(95)	0.21840(88)	2.43(37)
TWE1	160×16^3	1.217468	710	2	–	–	–	–

Table 1: List of lattices used in this study. $\langle P \rangle$ is the average value of the plaquette, τ is its integrated
autocorrelation time; λ is the lowest eigenvalue of the Hermitian Dirac matrix squared H^2, and again τ_λ is
the corresponding autocorrelation time. The bare mass for the TWE1 lattice is tuned to the chiral limit.

2.1 Observables

Mesonic observables are extracted from two-point functions of fermion bilinears:

$$f_{\Gamma\Gamma'}(t) = \sum_{\vec{x}} \left\langle \Phi_\Gamma(\vec{x},t)^\dagger \Phi_{\Gamma'}(\vec{0},0) \right\rangle, \qquad (2.1)$$

where

$$\Phi_\Gamma(\vec{x},t) = \bar{\psi}_1(\vec{x},t)\Gamma\psi_2(\vec{x},t). \qquad (2.2)$$

Note that we always consider non-singlet flavor states, as indicated by the indices $1, 2$ that appear
in the definition of the fermion bilinear. The matrices Γ and Γ' act in spin space, and determine

the quantum numbers of the states that contribute to the correlator in Eq. (2.1). The details of the analysis used to extract the PCAC mass, the hadron masses, and the decay constants are explained in detail in the Appendix of Ref. [14].

Gluonic observables are obtained using a variational method and a large basis of operators, as described in Ref. [17].

2.2 Finite temperature effects

We had noticed in our previous simulations that lattices with a temporal extent $T/a = 16, 24$ are not long enough to identify unambiguously the onset of the asymptotic behaviour of the field correlators [14]. Larger time extensions have been used in this study in order to be able to identify long plateaux in the two-point correlators, and to fit the large time behaviour in a regime where contaminations from higher states in the spectrum are suppressed. A typical set of plateaux for the mass of the pseudoscalar meson is reported in Fig. 1. It is clear from the plot, that lattices with temporal extent $T/a \geq 64$ exhibit very clear plateaux, which can be easily fitted to a constant over a large range in t. As a consequence, we decided not to use smeared sources for this analysis, since the introduction of smeared sources increases the auto-correlation time of the spectral observables.
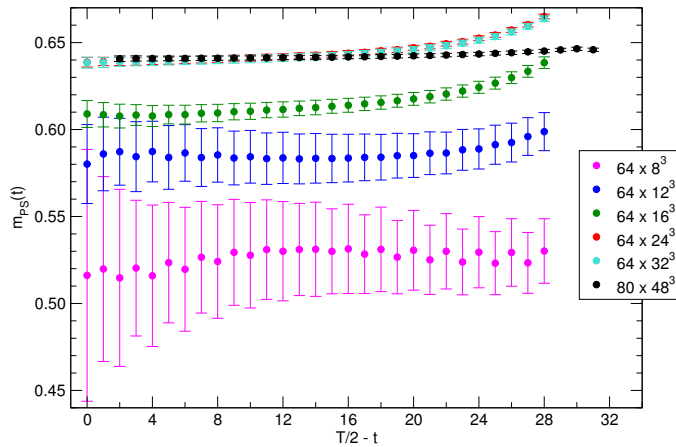
Figure 1: Plateaux for the effective mass in the PS channel at $\beta = 2.25$, and $am_0 = -1.15$. It is clear from the figure that the plateaux as a function of t are clearly identified for the current range of parameters, and that there is no contamination from higher states in the spectrum for the lattices considered here, ie with $T/a \geq 64$.

3. Results

The heaviest fermion mass in the new set of simulations is $am_0 = -1.05$, which corresponds to a PCAC mass of $am = 0.2688(15)$. The full spectrum is shown in Fig. 2. As observed in previous studies the mesons are heavier than the glueballs, with the smallest scale being set by the string tension. At this value of the fermion mass, the finite volume effects on the mesonic states are small, and we can confidently extrapolate their values to the thermodynamical limit. Different combinations of Γ, Γ' that project onto the same physical states yield results that are compatible
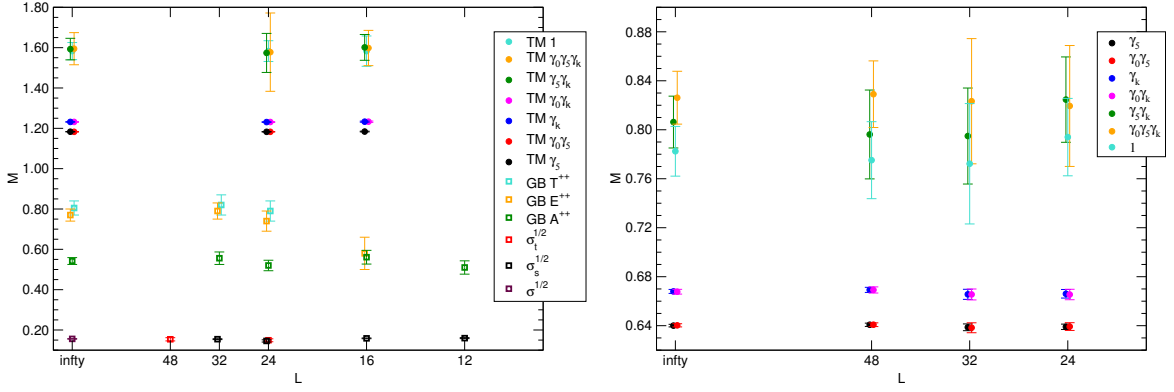
Figure 2: Summary of the spectrum for all the states included in this analysis at $am_0 = -1.05$ (left) and $am_0 = -1.15$ (right). The data are shown as a function of the number of sites in the spatial directions L/a.

within statistical errors. The new simulations confirm the results that we presented in previous studies [14]. For the string tension we see a discrepancy between the value of the string tension computed on the smaller lattices, and the one obtained on the larger volumes. Simulations on sufficiently large lattices, $L/a \geq 24$ yield consistent results between the spatial and temporal string tensions.

Finite volume effects are more significant for the lighter fermion mass. It is clear from Fig. 1 that the mass of the pseudoscalar is affected by sizeable finite volume corrections on the smaller lattices. The fitted value converges for lattices with $L/a \geq 24$. It is clear from this plot, that the masses are affected by large finite-volume effects on the smaller lattices, and that the effective mass is growing as the spatial size of the lattice increased. This is consistent with the observation that, in a theory where chiral symmetry is not spontaneously broken, the pseudoscalar mass reaches the infinite volume limit from below, as explained in Ref. [18, 19].

The plateaux in the effective mass of the pseudoscalar also show that a large temporal extent is needed in order to suppress the corrections from heavier states in the same channel. This is expected for a mass deformed conformal theory, since *all* the states in the spectrum should scale to zero following the same power-law scaling formula. The contribution from excited states becomes neglibile when:

$$t\Delta M_{\mathrm{PS}} \gg 1 \tag{3.1}$$

where ΔM_{PS} is the mass difference between the ground state and the first excited stated in the pseudoscalar channel. For a conformal theory near the chiral limit, $\Delta M_{\mathrm{PS}} \propto M_{\mathrm{PS}}$, so that the exponential suppression of the excited states becomes really effective only at large temporal separations.

Data for the mesonic spectrum at $am_0 = -1.15$ are displayed in Fig. 2, showing that a reliable extrapolation to the infinite-volume limit is possible using data for lattices with $L/a \geq 24$. This conclusion is supported by the observed independence of the mesonic spectrum form the choice of boundary conditions for $L/a \geq 24$. Note that for this choice of the bare fermion mass, the PCAC mass is $am = 0.11792(63)$.

The time-history of the topological charge along the HMC evolution is shown in Fig. 3. The topological charge is computed using a bosonic estimator for different values of the Wilson flow

time t. With parameters currently in use, the HMC seems to sample the topology correctly. A more detailed investigation of these issues is required.
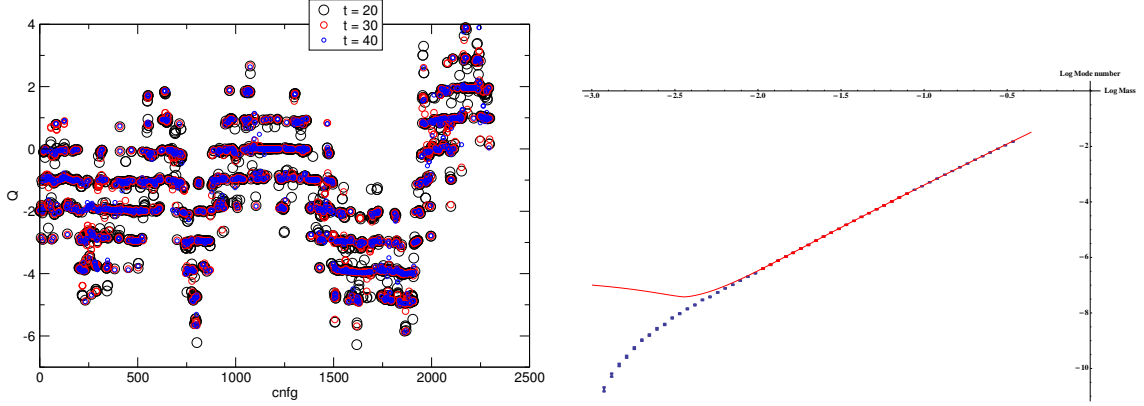
Figure 3: Time history for the topological charge as a function of the configuration number along the HMC evolution. Values for different values of the Wilson flow time are reported (**Left**). Mode number for the Dirac operator as a function of the measured on the lattice TWE1. The curve shows a fit to the predicted scaling behaviour. These results are preliminary (**Right**).

The density of eigenvalues of the Dirac operator has proved to be a valuable tool to measure the mass anomalous dimension in a conformal theory [20, 21, 22]. Using the techniques implemented in Ref. [22], we have measured the density of eigenvalues on the twisted lattices. Denoting by $\rho(\omega)$ the eigenvalue density for the operator $(D+m)^\dagger(D+m)$, the mode number is defined as

$$\nu(M) = 2 \int_0^{\sqrt{M^2-m^2}} d\omega\,\rho(\omega). \tag{3.2}$$

The expected scaling is dictated by the mass anomalous dimension:

$$a^{-4}\nu(M) = a^{-4}\nu_0 + A\left[(aM)^2 - (am)^2\right]^{\frac{2}{1+\gamma^*}}. \tag{3.3}$$

The results for the lattice TWE1 are shown in Fig. 3. As expected on theoretical grounds, an intermediate region in the value of the mode number can be identified where a power-law yields an excellent fit to the data. The fit yields a determination of the mass anamalous dimension

$$\gamma_* = 0.38(2), \tag{3.4}$$

in agreement with the value obtained in Ref. [22]. These preliminary results are encouraging, and will be finalised in a forthcoming work.

4. Outlook

Our latest simulations show convincingly that finite volume effects can be kept under control in the spectrum of MWT. The analysis for the glueball spectrum is being finalised, and we expect to have a determination of the whole spectrum with controlled systematics. We have started to monitor the topology, in order to verify that our simulations are not stuck at fixed topology. Last but not

least, we have looked at the eigenvalue density, and computed the mass anomalous dimension on one of the lattices with twisted boundary conditions. The twisted boundary conditions allow us to simulate at very small fermion mass, and our analysis confirms the results obtained on periodic lattices in earlier studies.

The preliminary results reported here are in agreement with our previous findings for this model, a comprehensive report of these results is in preparation.

References

[1] J. Kuti, plenary tak, these proceedings.

[2] D. K. Hong, S. D. H. Hsu and F. Sannino, Phys. Lett. B **597**, 89 (2004) [hep-ph/0406200].

[3] Z. Fodor, K. Holland, J. Kuti, D. Nogradi, C. Schroeder and C. H. Wong, Phys. Lett. B **718**, 657 (2012) [arXiv:1209.0391 [hep-lat]].

[4] T. Appelquist, R. Babich, R. C. Brower, M. I. Buchoff, M. Cheng, M. A. Clark, S. D. Cohen and G. T. Fleming *et al.*, Phys. Rev. D **85**, 074505 (2012) [arXiv:1201.3977 [hep-lat]].

[5] K. -I. Ishikawa, Y. Iwasaki, Y. Nakayama and T. Yoshie, arXiv:1310.5049 [hep-lat].

[6] M. A. Luty and T. Okui, JHEP **0609**, 070 (2006) [hep-ph/0409274].

[7] K. Yamawaki, M. Bando and K. -i. Matumoto, Phys. Rev. Lett. **56**, 1335 (1986).

[8] R. Rattazzi, V. S. Rychkov, E. Tonni and A. Vichi, JHEP **0812**, 031 (2008) [arXiv:0807.0004 [hep-th]].

[9] D. Elander and M. Piai, Nucl. Phys. B **867**, 779 (2013) [arXiv:1208.0546 [hep-ph]].

[10] D. D. Dietrich, F. Sannino and K. Tuominen, Phys. Rev. D **72**, 055001 (2005) [hep-ph/0505059].

[11] L. Del Debbio, B. Lucini, A. Patella, C. Pica and A. Rago, Phys. Rev. D **82**, 014510 (2010) [arXiv:1004.3206 [hep-lat]].

[12] A. J. Hietanen, K. Rummukainen and K. Tuominen, Phys. Rev. D **80**, 094504 (2009) [arXiv:0904.0864 [hep-lat]].

[13] F. Bursa, L. Del Debbio, L. Keegan, C. Pica and T. Pickup, Phys. Rev. D **81**, 014505 (2010) [arXiv:0910.4535 [hep-ph]].

[14] F. Bursa, L. Del Debbio, D. Henty, E. Kerrane, B. Lucini, A. Patella, C. Pica and T. Pickup *et al.*, Phys. Rev. D **84**, 034506 (2011) [arXiv:1104.4301 [hep-lat]].

[15] L. Del Debbio, A. Patella and C. Pica, Phys. Rev. D **81**, 094503 (2010) [arXiv:0805.2058 [hep-lat]].

[16] G. 't Hooft, Nucl. Phys. B **153**, 141 (1979).

[17] B. Lucini, A. Rago and E. Rinaldi, JHEP **1008**, 119 (2010) [arXiv:1007.3879 [hep-lat]].

[18] A. Patella, L. Del Debbio, B. Lucini, C. Pica and A. Rago, PoS LATTICE **2011**, 084 (2011) [arXiv:1111.4672 [hep-lat]].

[19] M. Luscher, Commun. Math. Phys. **104**, 177 (1986).

[20] T. DeGrand, Phys. Rev. D **80**, 114507 (2009) [arXiv:0910.3072 [hep-lat]].

[21] L. Del Debbio and R. Zwicky, Phys. Rev. D **82**, 014502 (2010) [arXiv:1005.2371 [hep-ph]].

[22] A. Patella, Phys. Rev. D **86**, 025006 (2012) [arXiv:1204.4432 [hep-lat]].